Measurement of the Λ_b^0 Lifetime Using Semileptonic Decays

V. M. Abazov,[35] B. Abbott,[75] M. Abolins,[65] B. S. Acharya,[28] M. Adams,[51] T. Adams,[49] E. Aguilo,[5] S. H. Ahn,[30] M. Ahsan,[59] G. D. Alexeev,[35] G. Alkhazov,[39] A. Alton,[64,*] G. Alverson,[63] G. A. Alves,[2] M. Anastasoaie,[34] L. S. Ancu,[34] T. Andeen,[53] S. Anderson,[45] B. Andrieu,[16] M. S. Anzelc,[53] Y. Arnoud,[13] M. Arov,[60] M. Arthaud,[17] A. Askew,[49] B. Åsman,[40] A. C. S. Assis Jesus,[3] O. Atramentov,[49] C. Autermann,[20] C. Avila,[7] C. Ay,[23] F. Badaud,[12] A. Baden,[61] L. Bagby,[52] B. Baldin,[50] D. V. Bandurin,[59] S. Banerjee,[28] P. Banerjee,[28] E. Barberis,[63] A.-F. Barfuss,[14] P. Bargassa,[80] P. Baringer,[58] J. Barreto,[2] J. F. Bartlett,[50] U. Bassler,[16] D. Bauer,[43] S. Beale,[5] A. Bean,[58] M. Begalli,[3] M. Begel,[71] C. Belanger-Champagne,[40] L. Bellantoni,[50] A. Bellavance,[50] J. A. Benitez,[65] S. B. Beri,[26] G. Bernardi,[16] R. Bernhard,[22] L. Berntzon,[14] I. Bertram,[42] M. Besançon,[17] R. Beuselinck,[43] V. A. Bezzubov,[38] P. C. Bhat,[50] V. Bhatnagar,[26] C. Biscarat,[19] G. Blazey,[52] F. Blekman,[43] S. Blessing,[49] D. Bloch,[18] K. Bloom,[67] A. Boehnlein,[50] D. Boline,[62] T. A. Bolton,[59] G. Borissov,[42] K. Bos,[33] T. Bose,[77] A. Brandt,[78] R. Brock,[65] G. Brooijmans,[70] A. Bross,[50] D. Brown,[78] N. J. Buchanan,[49] D. Buchholz,[53] M. Buehler,[81] V. Buescher,[21] S. Burdin,[42,†] S. Burke,[45] T. H. Burnett,[82] C. P. Buszello,[43] J. M. Butler,[62] P. Calfayan,[24] S. Calvet,[14] J. Cammin,[71] S. Caron,[33] W. Carvalho,[3] B. C. K. Casey,[77] N. M. Cason,[55] H. Castilla-Valdez,[32] S. Chakrabarti,[17] D. Chakraborty,[52] K. M. Chan,[55] K. Chan,[5] A. Chandra,[48] F. Charles,[18] E. Cheu,[45] F. Chevallier,[13] D. K. Cho,[62] S. Choi,[31] B. Choudhary,[27] L. Christofek,[77] T. Christoudias,[43] S. Cihangir,[50] D. Claes,[67] C. Clément,[40] B. Clément,[18] Y. Coadou,[5] M. Cooke,[80] W. E. Cooper,[50] M. Corcoran,[80] F. Couderc,[17] M.-C. Cousinou,[14] S. Crépé-Renaudin,[13] D. Cutts,[77] M. Ćwiok,[29] H. da Motta,[2] A. Das,[62] G. Davies,[43] K. De,[78] S. J. de Jong,[34] P. de Jong,[33] E. De La Cruz-Burelo,[64] C. De Oliveira Martins,[3] J. D. Degenhardt,[64] F. Déliot,[17] M. Demarteau,[50] R. Demina,[71] D. Denisov,[50] S. P. Denisov,[38] S. Desai,[50] H. T. Diehl,[50] M. Diesburg,[50] A. Dominguez,[67] H. Dong,[72] L. V. Dudko,[37] L. Duflot,[15] S. R. Dugad,[28] D. Duggan,[49] A. Duperrin,[14] J. Dyer,[65] A. Dyshkant,[52] M. Eads,[67] D. Edmunds,[65] J. Ellison,[48] V. D. Elvira,[50] Y. Enari,[77] S. Eno,[61] P. Ermolov,[37] H. Evans,[54] A. Evdokimov,[73] V. N. Evdokimov,[38] A. V. Ferapontov,[59] T. Ferbel,[71] F. Fiedler,[24] F. Filthaut,[34] W. Fisher,[50] H. E. Fisk,[50] M. Ford,[44] M. Fortner,[52] H. Fox,[22] S. Fu,[50] S. Fuess,[50] T. Gadfort,[82] C. F. Galea,[34] E. Gallas,[50] E. Galyaev,[55] C. Garcia,[71] A. Garcia-Bellido,[82] V. Gavrilov,[36] P. Gay,[12] W. Geist,[18] D. Gelé,[18] C. E. Gerber,[51] Y. Gershtein,[49] D. Gillberg,[5] G. Ginther,[71] N. Gollub,[40] B. Gómez,[7] A. Goussiou,[55] P. D. Grannis,[72] H. Greenlee,[50] Z. D. Greenwood,[60] E. M. Gregores,[4] G. Grenier,[19] Ph. Gris,[12] J.-F. Grivaz,[15] A. Grohsjean,[24] S. Grünendahl,[50] M. W. Grünewald,[29] J. Guo,[72] F. Guo,[72] P. Gutierrez,[75] G. Gutierrez,[50] A. Haas,[70] N. J. Hadley,[61] P. Haefner,[24] S. Hagopian,[49] J. Haley,[68] I. Hall,[75] R. E. Hall,[47] L. Han,[6] K. Hanagaki,[50] P. Hansson,[40] K. Harder,[44] A. Harel,[71] R. Harrington,[63] J. M. Hauptman,[57] R. Hauser,[65] J. Hays,[43] T. Hebbeker,[20] D. Hedin,[52] J. G. Hegeman,[33] J. M. Heinmiller,[51] A. P. Heinson,[48] U. Heintz,[62] C. Hensel,[58] K. Herner,[72] G. Hesketh,[63] M. D. Hildreth,[55] R. Hirosky,[81] J. D. Hobbs,[72] B. Hoeneisen,[11] H. Hoeth,[25] M. Hohlfeld,[21] S. J. Hong,[30] R. Hooper,[77] S. Hossain,[75] P. Houben,[33] Y. Hu,[72] Z. Hubacek,[9] V. Hynek,[8] I. Iashvili,[69] R. Illingworth,[50] A. S. Ito,[50] S. Jabeen,[62] M. Jaffré,[15] S. Jain,[75] K. Jakobs,[22] C. Jarvis,[61] R. Jesik,[43] K. Johns,[45] C. Johnson,[70] M. Johnson,[50] A. Jonckheere,[50] P. Jonsson,[43] A. Juste,[50] D. Käfer,[20] S. Kahn,[73] E. Kajfasz,[14] A. M. Kalinin,[35] J. R. Kalk,[65] J. M. Kalk,[60] S. Kappler,[20] D. Karmanov,[37] J. Kasper,[62] P. Kasper,[50] I. Katsanos,[70] D. Kau,[49] R. Kaur,[26] V. Kaushik,[78] R. Kehoe,[79] S. Kermiche,[14] N. Khalatyan,[38] A. Khanov,[76] A. Kharchilava,[69] Y. M. Kharzheev,[35] D. Khatidze,[70] H. Kim,[31] T. J. Kim,[30] M. H. Kirby,[34] M. Kirsch,[20] B. Klima,[50] J. M. Kohli,[26] J.-P. Konrath,[22] M. Kopal,[75] V. M. Korablev,[38] B. Kothari,[70] A. V. Kozelov,[38] D. Krop,[54] A. Kryemadhi,[81] T. Kuhl,[23] A. Kumar,[69] S. Kunori,[61] A. Kupco,[10] T. Kurča,[19] J. Kvita,[8] F. Lacroix,[12] D. Lam,[55] S. Lammers,[70] G. Landsberg,[77] J. Lazoflores,[49] P. Lebrun,[19] W. M. Lee,[50] A. Leflat,[37] F. Lehner,[41] J. Lellouch,[16] V. Lesne,[12] J. Leveque,[45] M. Lewin,[42] P. Lewis,[43] J. Li,[78] Q. Z. Li,[50] L. Li,[48] S. M. Lietti,[4] J. G. R. Lima,[52] D. Lincoln,[50] J. Linnemann,[65] V. V. Lipaev,[38] R. Lipton,[50] Y. Liu,[6] Z. Liu,[5] L. Lobo,[43] A. Lobodenko,[39] M. Lokajicek,[10] A. Lounis,[18] P. Love,[42] H. J. Lubatti,[82] A. L. Lyon,[50] A. K. A. Maciel,[2] D. Mackin,[80] R. J. Madaras,[46] P. Mättig,[25] C. Magass,[20] A. Magerkurth,[64] N. Makovec,[15] P. K. Mal,[55] H. B. Malbouisson,[3] S. Malik,[67] V. L. Malyshev,[35] H. S. Mao,[50] Y. Maravin,[59] B. Martin,[13] R. McCarthy,[72] A. Melnitchouk,[66] A. Mendes,[14] L. Mendoza,[7] P. G. Mercadante,[4] M. Merkin,[37] K. W. Merritt,[50] J. Meyer,[21] A. Meyer,[20] M. Michaut,[17] T. Millet,[19] J. Mitrevski,[70] J. Molina,[3] R. K. Mommsen,[44] N. K. Mondal,[28] R. W. Moore,[5] T. Moulik,[58] G. S. Muanza,[19] M. Mulders,[50] M. Mulhearn,[70] O. Mundal,[21] L. Mundim,[3] E. Nagy,[14] M. Naimuddin,[50] M. Narain,[77] N. A. Naumann,[34] H. A. Neal,[64] J. P. Negret,[7] P. Neustroev,[39] H. Nilsen,[22] A. Nomerotski,[50] S. F. Novaes,[4] T. Nunnemann,[24] V. O'Dell,[50] D. C. O'Neil,[5] G. Obrant,[39] C. Ochando,[15] D. Onoprienko,[59] N. Oshima,[50] J. Osta,[55] R. Otec,[9] G. J. Otero y Garzón,[51] M. Owen,[44] P. Padley,[80] M. Pangilinan,[77] N. Parashar,[56] S.-J. Park,[71] S. K. Park,[30] J. Parsons,[70] R. Partridge,[77] N. Parua,[54] A. Patwa,[73] G. Pawloski,[80] B. Penning,[22]

P. M. Perea,[48] K. Peters,[44] Y. Peters,[25] P. Pétroff,[15] M. Petteni,[43] R. Piegaia,[1] J. Piper,[65] M.-A. Pleier,[21] P. L. M. Podesta-Lerma,[32,‡] V. M. Podstavkov,[50] Y. Pogorelov,[55] M.-E. Pol,[2] P. Polozov,[36] A. Pompoš,[75] B. G. Pope,[65] A. V. Popov,[38] C. Potter,[5] W. L. Prado da Silva,[3] H. B. Prosper,[49] S. Protopopescu,[73] J. Qian,[64] A. Quadt,[21] B. Quinn,[66] A. Rakitine,[42] M. S. Rangel,[2] K. J. Rani,[28] K. Ranjan,[27] P. N. Ratoff,[42] P. Renkel,[79] S. Reucroft,[63] P. Rich,[44] M. Rijssenbeek,[72] I. Ripp-Baudot,[18] F. Rizatdinova,[76] S. Robinson,[43] R. F. Rodrigues,[3] C. Royon,[17] P. Rubinov,[50] R. Ruchti,[55] G. Safronov,[36] G. Sajot,[13] A. Sánchez-Hernández,[32] M. P. Sanders,[16] A. Santoro,[3] G. Savage,[50] L. Sawyer,[60] T. Scanlon,[43] D. Schaile,[24] R. D. Schamberger,[72] Y. Scheglov,[39] H. Schellman,[53] P. Schieferdecker,[24] T. Schliephake,[25] C. Schmitt,[25] C. Schwanenberger,[44] A. Schwartzman,[68] R. Schwienhorst,[65] J. Sekaric,[49] S. Sengupta,[49] H. Severini,[75] E. Shabalina,[51] M. Shamim,[59] V. Shary,[17] A. A. Shchukin,[38] R. K. Shivpuri,[27] D. Shpakov,[50] V. Siccardi,[18] V. Simak,[9] V. Sirotenko,[50] P. Skubic,[75] P. Slattery,[71] D. Smirnov,[55] R. P. Smith,[50] J. Snow,[74] G. R. Snow,[67] S. Snyder,[73] S. Söldner-Rembold,[44] L. Sonnenschein,[16] A. Sopczak,[42] M. Sosebee,[78] K. Soustruznik,[8] M. Souza,[2] B. Spurlock,[78] J. Stark,[13] J. Steele,[60] V. Stolin,[36] A. Stone,[51] D. A. Stoyanova,[38] J. Strandberg,[64] S. Strandberg,[40] M. A. Strang,[69] M. Strauss,[75] E. Strauss,[72] R. Ströhmer,[24] D. Strom,[53] M. Strovink,[46] L. Stutte,[50] S. Sumowidagdo,[49] P. Svoisky,[55] A. Sznajder,[3] M. Talby,[14] P. Tamburello,[45] A. Tanasijczuk,[1] W. Taylor,[5] P. Telford,[44] J. Temple,[45] B. Tiller,[24] F. Tissandier,[12] M. Titov,[17] V. V. Tokmenin,[35] M. Tomoto,[50] T. Toole,[61] I. Torchiani,[22] T. Trefzger,[23] D. Tsybychev,[72] B. Tuchming,[17] C. Tully,[68] P. M. Tuts,[70] R. Unalan,[65] S. Uvarov,[39] L. Uvarov,[39] S. Uzunyan,[52] B. Vachon,[5] P. J. van den Berg,[33] B. van Eijk,[33] R. Van Kooten,[54] W. M. van Leeuwen,[33] N. Varelas,[51] E. W. Varnes,[45] A. Vartapetian,[78] I. A. Vasilyev,[38] M. Vaupel,[25] P. Verdier,[19] L. S. Vertogradov,[35] M. Verzocchi,[50] F. Villeneuve-Seguier,[43] P. Vint,[43] P. Vokac,[9] E. Von Toerne,[59] M. Voutilainen,[67,§] M. Vreeswijk,[33] R. Wagner,[68] H. D. Wahl,[49] L. Wang,[61] M. H. L. S Wang,[50] J. Warchol,[55] G. Watts,[82] M. Wayne,[55] M. Weber,[50] G. Weber,[23] H. Weerts,[65] A. Wenger,[22,‖] N. Wermes,[21] M. Wetstein,[61] A. White,[78] D. Wicke,[25] G. W. Wilson,[58] S. J. Wimpenny,[48] M. Wobisch,[60] D. R. Wood,[63] T. R. Wyatt,[44] Y. Xie,[77] S. Yacoob,[53] R. Yamada,[50] M. Yan,[61] T. Yasuda,[50] Y. A. Yatsunenko,[35] K. Yip,[73] H. D. Yoo,[77] S. W. Youn,[53] J. Yu,[78] C. Yu,[13] A. Yurkewicz,[72] A. Zatserklyaniy,[52] C. Zeitnitz,[25] D. Zhang,[50] T. Zhao,[82] B. Zhou,[64] J. Zhu,[72] M. Zielinski,[71] D. Zieminska,[54] A. Zieminski,[54] L. Zivkovic,[70] V. Zutshi,[52] and E. G. Zverev[37]

(D0 Collaboration)

[1]*Universidad de Buenos Aires, Buenos Aires, Argentina*
[2]*LAFEX, Centro Brasileiro de Pesquisas Físicas, Rio de Janeiro, Brazil*
[3]*Universidade do Estado do Rio de Janeiro, Rio de Janeiro, Brazil*
[4]*Instituto de Física Teórica, Universidade Estadual Paulista, São Paulo, Brazil*
[5]*University of Alberta, Edmonton, Alberta, Canada,*
Simon Fraser University, Burnaby, British Columbia, Canada,
York University, Toronto, Ontario, Canada, and McGill University, Montreal, Quebec, Canada
[6]*University of Science and Technology of China, Hefei, People's Republic of China*
[7]*Universidad de los Andes, Bogotá, Colombia*
[8]*Center for Particle Physics, Charles University, Prague, Czech Republic*
[9]*Czech Technical University, Prague, Czech Republic*
[10]*Center for Particle Physics, Institute of Physics, Academy of Sciences of the Czech Republic, Prague, Czech Republic*
[11]*Universidad San Francisco de Quito, Quito, Ecuador*
[12]*Laboratoire de Physique Corpusculaire, IN2P3-CNRS, Université Blaise Pascal, Clermont-Ferrand, France*
[13]*Laboratoire de Physique Subatomique et de Cosmologie, IN2P3-CNRS, Universite de Grenoble 1, Grenoble, France*
[14]*CPPM, IN2P3-CNRS, Université de la Méditerranée, Marseille, France*
[15]*Laboratoire de l'Accélérateur Linéaire, IN2P3-CNRS et Université Paris-Sud, Orsay, France*
[16]*LPNHE, IN2P3-CNRS, Universités Paris VI and VII, Paris, France*
[17]*DAPNIA/Service de Physique des Particules, CEA, Saclay, France*
[18]*IPHC, Université Louis Pasteur et Université de Haute Alsace, CNRS, IN2P3, Strasbourg, France*
[19]*IPNL, Université Lyon 1, CNRS/IN2P3, Villeurbanne, France and Université de Lyon, Lyon, France*
[20]*III. Physikalisches Institut A, RWTH Aachen, Aachen, Germany*
[21]*Physikalisches Institut, Universität Bonn, Bonn, Germany*
[22]*Physikalisches Institut, Universität Freiburg, Freiburg, Germany*
[23]*Institut für Physik, Universität Mainz, Mainz, Germany*
[24]*Ludwig-Maximilians-Universität München, München, Germany*
[25]*Fachbereich Physik, University of Wuppertal, Wuppertal, Germany*
[26]*Panjab University, Chandigarh, India*
[27]*Delhi University, Delhi, India*

[28]*Tata Institute of Fundamental Research, Mumbai, India*
[29]*University College Dublin, Dublin, Ireland*
[30]*Korea Detector Laboratory, Korea University, Seoul, Korea*
[31]*SungKyunKwan University, Suwon, Korea*
[32]*CINVESTAV, Mexico City, Mexico*
[33]*FOM-Institute NIKHEF and University of Amsterdam/NIKHEF, Amsterdam, The Netherlands*
[34]*Radboud University Nijmegen/NIKHEF, Nijmegen, The Netherlands*
[35]*Joint Institute for Nuclear Research, Dubna, Russia*
[36]*Institute for Theoretical and Experimental Physics, Moscow, Russia*
[37]*Moscow State University, Moscow, Russia*
[38]*Institute for High Energy Physics, Protvino, Russia*
[39]*Petersburg Nuclear Physics Institute, St. Petersburg, Russia*
[40]*Lund University, Lund, Sweden, Royal Institute of Technology and Stockholm University, Stockholm, Sweden, and Uppsala University, Uppsala, Sweden*
[41]*Physik Institut der Universität Zürich, Zürich, Switzerland*
[42]*Lancaster University, Lancaster, United Kingdom*
[43]*Imperial College, London, United Kingdom*
[44]*University of Manchester, Manchester, United Kingdom*
[45]*University of Arizona, Tucson, Arizona 85721, USA*
[46]*Lawrence Berkeley National Laboratory and University of California, Berkeley, California 94720, USA*
[47]*California State University, Fresno, California 93740, USA*
[48]*University of California, Riverside, California 92521, USA*
[49]*Florida State University, Tallahassee, Florida 32306, USA*
[50]*Fermi National Accelerator Laboratory, Batavia, Illinois 60510, USA*
[51]*University of Illinois at Chicago, Chicago, Illinois 60607, USA*
[52]*Northern Illinois University, DeKalb, Illinois 60115, USA*
[53]*Northwestern University, Evanston, Illinois 60208, USA*
[54]*Indiana University, Bloomington, Indiana 47405, USA*
[55]*University of Notre Dame, Notre Dame, Indiana 46556, USA*
[56]*Purdue University Calumet, Hammond, Indiana 46323, USA*
[57]*Iowa State University, Ames, Iowa 50011, USA*
[58]*University of Kansas, Lawrence, Kansas 66045, USA*
[59]*Kansas State University, Manhattan, Kansas 66506, USA*
[60]*Louisiana Tech University, Ruston, Louisiana 71272, USA*
[61]*University of Maryland, College Park, Maryland 20742, USA*
[62]*Boston University, Boston, Massachusetts 02215, USA*
[63]*Northeastern University, Boston, Massachusetts 02115, USA*
[64]*University of Michigan, Ann Arbor, Michigan 48109, USA*
[65]*Michigan State University, East Lansing, Michigan 48824, USA*
[66]*University of Mississippi, University, Mississippi 38677, USA*
[67]*University of Nebraska, Lincoln, Nebraska 68588, USA*
[68]*Princeton University, Princeton, New Jersey 08544, USA*
[69]*State University of New York, Buffalo, New York 14260, USA*
[70]*Columbia University, New York, New York 10027, USA*
[71]*University of Rochester, Rochester, New York 14627, USA*
[72]*State University of New York, Stony Brook, New York 11794, USA*
[73]*Brookhaven National Laboratory, Upton, New York 11973, USA*
[74]*Langston University, Langston, Oklahoma 73050, USA*
[75]*University of Oklahoma, Norman, Oklahoma 73019, USA*
[76]*Oklahoma State University, Stillwater, Oklahoma 74078, USA*
[77]*Brown University, Providence, Rhode Island 02912, USA*
[78]*University of Texas, Arlington, Texas 76019, USA*
[79]*Southern Methodist University, Dallas, Texas 75275, USA*
[80]*Rice University, Houston, Texas 77005, USA*
[81]*University of Virginia, Charlottesville, Virginia 22901, USA*
[82]*University of Washington, Seattle, Washington 98195, USA*

(Received 18 June 2007; published 30 October 2007)

We report a measurement of the Λ_b^0 lifetime using a sample corresponding to 1.3 fb^{-1} of data collected by the D0 experiment in 2002–2006 during run II of the Fermilab Tevatron collider. The Λ_b^0 baryon is reconstructed via the decay $\Lambda_b^0 \to \mu\bar{\nu}\Lambda_c^+ X$. Using 4437 ± 329 signal candidates, we measure the Λ_b^0

lifetime to be $\tau(\Lambda_b^0) = 1.290^{+0.119}_{-0.110}(\text{stat})^{+0.087}_{-0.091}(\text{syst})$ ps, which is among the most precise measurements in semileptonic Λ_b^0 decays. This result is in good agreement with the world average value.

DOI: 10.1103/PhysRevLett.99.182001 PACS numbers: 14.20.Mr, 13.30.Ce

The lifetimes of b hadrons provide an important test of models describing quark interaction within bound states. The experimental measurements of the lifetimes are in reasonable agreement with the theoretical predictions [1–4], but further improvement in the experimental and theoretical precision is essential for the development of quantum chromodynamics.

The lifetime of b hadrons has recently attracted special interest. The PDG-2006 world average Λ_b^0 lifetime is $\tau(\Lambda_b^0) = 1.230 \pm 0.074$ ps, and the ratio of the Λ_b^0 baryon and B^0 meson lifetimes is $\tau(\Lambda_b^0)/\tau(B^0) = 0.80 \pm 0.05$ [5], in good agreement with the theoretical prediction $\tau(\Lambda_b^0)/\tau(B^0) = 0.86 \pm 0.05$ [4]. However, the Λ_b^0 lifetime measurement from the CDF collaboration in the $\Lambda_b^0 \to J/\psi\Lambda$ decay gives a significantly larger value: $\tau(\Lambda_b^0) = 1.593^{+0.083}_{-0.078} \pm 0.033$ ps [6]. The D0 measurement in the same decay gives a value consistent with the PDG-2006 world average: $\tau(\Lambda_b^0) = 1.218^{+0.130}_{-0.115} \pm 0.042$ ps [7]. These two results are not included in the quoted world average. Additional Λ_b^0 lifetime measurements could provide a potential resolution of this inconsistency.

This Letter presents a measurement of the Λ_b^0 lifetime using the semileptonic decay $\Lambda_b^0 \to \mu\bar{\nu}\Lambda_c^+ X$, where X is any other particle. Charge conjugated states are implied throughout this Letter. The Λ_c^+ baryon is selected in the decay $\Lambda_c^+ \to K_S^0 p$. The sample corresponds to approximately 1.3 fb^{-1} of data collected by the D0 experiment in run II of the Fermilab Tevatron Collider.

The D0 detector is described in detail elsewhere [8]. The components most important to this analysis are the central tracking and muon systems. The central tracking system consists of a silicon microstrip tracker and a central fiber tracker, both located within a 2 T superconducting solenoidal magnet, with designs optimized for tracking and vertexing at pseudorapidities $|\eta| < 3$ and $|\eta| < 2.5$, respectively, (where $\eta = -\ln[\tan(\theta/2)]$ and θ is the polar angle of the particle with respect to the proton beam direction). The muon system is located outside the calorimeters and has pseudorapidity coverage $|\eta| < 2$. It consists of a layer of tracking detectors and scintillation trigger counters in front of 1.8 T iron toroids, followed by two similar layers after the toroids [9]. The trigger system identifies events of interest in a high-luminosity environment based on muon identification and charged tracking. Some triggers require a large impact parameter for the muon. Since this condition biases the lifetime measurement, the events selected exclusively by these triggers are removed from our sample. All processes and decays required for this analysis are simulated using the EVTGEN [10] generator interfaced to PYTHIA [11] and followed by full modeling of the detector response using GEANT [12] and event reconstruction.

Reconstruction of the Λ_b^0 decay starts from the selection of a muon, which must have at least two track segments in the muon chambers associated with a central track, with transverse momentum with respect to the beam axis $p_T > 2.0$ GeV/c. All charged particles in the event are clustered into jets using the Durham clustering algorithm [13]. The products of the Λ_c^+ decay are then searched for among tracks belonging to the jet containing the identified muon.

The primary vertex is determined using the method described in Ref. [14]. The K_S^0 meson is reconstructed as a combination of two oppositely charged tracks that have a common vertex displaced from the $p\bar{p}$ interaction point by at least 4 standard deviations of the measured decay length in the plane perpendicular to the beam direction. Both tracks are assigned the pion mass and the mass of the $\pi^+\pi^-$ system is required to be consistent with the K_S^0 mass to within 1.8 standard deviations. Any other charged track in the jet with $p_T > 1.0$ GeV/c and at least two hits in the silicon detector is assigned the proton mass and combined with the neutral extrapolated K_S^0 candidate to form a Λ_c^+ candidate. The Λ_c^+ candidate is combined with the muon to make a Λ_b^0 candidate, and its invariant mass is required to be between 3.4 and 5.4 GeV/c^2. The transverse distance d_T^{bc} between the Λ_b^0 and Λ_c^+ vertices is calculated and is assigned a positive sign if the Λ_b^0 vertex is closer to the primary vertex, and a negative sign otherwise. The Λ_b^0 candidate is required to have $-3.0 < d_T^{bc}/\sigma(d_T^{bc}) < 3.3$, where $\sigma(d_T^{bc})$ is the uncertainty of the d_T^{bc} measurement. The upper bound on the distance between the Λ_b^0 and Λ_c^+ vertices reduces the background significantly, since the Λ_c^+ lifetime is known to be very small: 0.200 ± 0.006 ps [5]. These selection criteria were chosen to optimize the signal to background ratio while avoiding any lifetime bias.

To further improve the Λ_b^0 signal selection, a likelihood ratio method [15] is utilized. This method provides a simple way to combine many discriminating variables into a single variable with an increased power to separate signal and background. The variables chosen for this analysis are the Λ_b^0 isolation, the transverse momentum of the K_S^0, proton and Λ_c^+ candidates, and the mass of the $\mu\Lambda_c^+$ system. The isolation is defined as the fraction of the total momentum of charged particles within a cone around the $\mu\Lambda_c^+$ direction carried by the Λ_b^0 candidate. The cone is defined by the condition $\sqrt{(\Delta\eta)^2 + (\Delta\phi)^2} < 0.5$, where $\Delta\eta$ and $\Delta\phi$ are the difference in pseudorapidity and azimuthal angle from the direction of the Λ_b^0 candidate.

Figure 1 shows the invariant mass $M(K_S^0 p)$ for the selected Λ_b^0 candidates. The fit to this distribution is performed with a signal Gaussian function and a fourth-order polynomial function for the background. The Λ_c^+ signal contains 4437 ± 329(stat) events at a central mass of 2285.8 ± 1.7 MeV$/c^2$. The width of the mass peak is $\sigma = 20.6 \pm 1.7$ MeV$/c^2$, consistent with that observed in the simulation.

Simulation shows that the contribution from the $B_d \to K_S^0 \pi$ decay when a pion is assigned the proton mass has a broad $M(K_S^0 p)$ distribution with no excess in the Λ_c^+ mass region.

Since the final state is not fully reconstructed, the Λ_b^0 proper decay length cannot be determined. Instead, a measured visible proper decay length, λ^M, is computed as $\lambda^M = mc(\boldsymbol{L}_T \cdot \boldsymbol{p}_T(\mu\Lambda_c^+))/|\boldsymbol{p}_T(\mu\Lambda_c^+)|^2$. $\boldsymbol{L}_T$ is the vector from the primary vertex to the Λ_b^0 vertex in the plane perpendicular to the beams, $\boldsymbol{p}_T(\mu\Lambda_c^+)$ is the transverse momentum of the $\mu\Lambda_c^+$ system and $m = 5.624$ GeV$/c^2$ is taken as the Λ_b^0 mass [5].

To determine the Λ_b^0 lifetime, the selected sample is split into a number of λ^M bins. The mass distribution in each bin is fitted with a signal Gaussian and a fourth-order polynomial background. The position and width of the Gaussian are fixed to the values obtained from the fit of the entire sample (see Fig. 1). The Gaussian normalization and background parameters are allowed to float in the fit. The range of λ^M and the number of signal events fitted in each bin n_i together with its statistical uncertainty σ_i are shown in Table I.

The expected number of signal events in each bin, n_i^e, is given by $n_i^e = N_{\rm tot} \int_i f(\lambda^M) d\lambda^M$, where $N_{\rm tot}$ is the total number of $\mu\Lambda_c^+$ events, and $f(\lambda^M)$ is the probability density function (PDF) for λ^M. The integration is done within the range of a given bin.

In addition to $\Lambda_b^0 \to \mu\bar{\nu}\Lambda_c^+ X$ decays, the Λ_c^+ baryon can also be created in $c\bar{c}$ or $b\bar{b}$ production, along with a muon from the decay of the second c or b hadron. In what follows, these processes are referred to as *peaking background*, since they produce a Λ_c^+ peak in the $K_S^0 p$ mass spectrum imitating the signal. Such events are reconstructed as Λ_b^0 candidates, and have a fake vertex formed by the intersection of the muon and Λ_c^+ trajectories. The simulation shows that the distribution of λ^M for such a fake vertex has a mean of zero and a standard deviation of ≈ 150 μm.

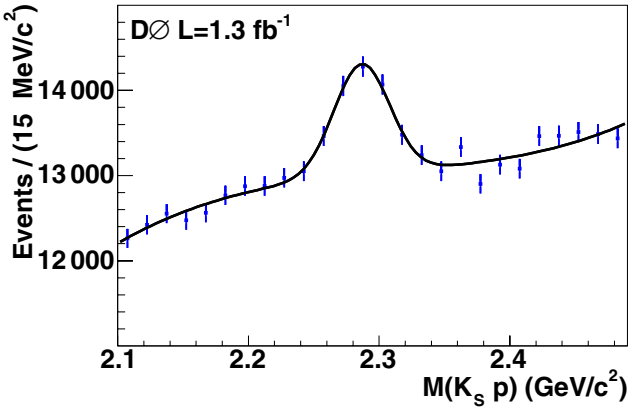

FIG. 1 (color online). The $K_S^0 p$ invariant mass for the selected Λ_b^0 candidates and fit overlaid (see text).

The expression for $f(\lambda^M)$ takes into account the contributions from signal and peaking background: $f(\lambda^M) = (1 - r_{\rm bck}) f_{\rm sig}(\lambda^M) + r_{\rm bck} f_{\rm bck}(\lambda^M)$. Here $r_{\rm bck}$ is the fraction of peaking background, and $f_{\rm sig}(\lambda^M)$ and $f_{\rm bck}(\lambda^M)$ are the PDFs for signal and background, respectively. The background PDF is taken from the simulation. The signal PDF is expressed as the convolution of the decay probability and the detector resolution: $f_{\rm sig}(\lambda^M) = \int dK H(K) \times \{\theta(\lambda) K/(c\tau) \exp[-K\lambda/(c\tau)] \otimes R(\lambda^M - \lambda, s)\}$. Here, τ is the Λ_b^0 lifetime, and $\theta(\lambda)$ is the step function. The factor $K = p_T(\mu\Lambda_c^+)/p_T(\Lambda_b^0)$ is a measure of the difference between the measured $p_T(\mu\Lambda_c^+)$ and true momentum of the Λ_b^0 candidate, and $H(K)$ is its PDF. The $R(\lambda^M - \lambda, s)$ is a function modeling the detector resolution. A scale factor s accounts for the difference between the expected and actual λ^M resolution.

The $H(K)$ distribution is obtained from the simulation. The contribution of decays $\Lambda_b^0 \to \mu\bar{\nu}\Lambda_c^+$ and $\Lambda_b^0 \to \mu\bar{\nu}\Sigma_c\pi$ with $\Sigma_c \to \Lambda_c^+\pi$ is taken into account. The contributions of $\Lambda_b^0 \to \Lambda_c^+ D_s^{(*)-}$ with the D_s^- decaying semileptonically, $\Xi_b \to \mu\bar{\nu}\Lambda_c X$ and $\Lambda_b^0 \to \tau^-\bar{\nu}\Lambda_c^+$ with $\tau^- \to \mu^-\bar{\nu}_\mu\nu_\tau$ are found to be strongly suppressed by the branching fractions and low reconstruction efficiency. To obtain $H(K)$, the K factor distribution of each process is weighted with its expected fraction in the selected sample. This is computed taking into account both the reconstruction efficiency and the branching fraction of each process. The fraction of $\ell^-\bar{\nu}\Lambda_c^+$ in semileptonic Λ_b^0 decays has been measured recently to be $0.47^{+0.12}_{-0.10}$ [5]. We use this result in our analysis.

The resolution function is given by $R(\lambda^M - \lambda, s) = \int f_{\rm res}(\sigma) G(\lambda^M - \lambda, \sigma, s) d\sigma$, where $f_{\rm res}(\sigma)$ is the PDF

TABLE I. Fitted signal yield in different λ^M bins.

λ^M range (cm)	Number of signal candidates $n_i \pm \sigma_i$ (stat)
$[-0.06, -0.04]$	62 ± 48
$[-0.04, -0.02]$	66 ± 69
$[-0.02, 0.00]$	587 ± 156
$[0.00, 0.02]$	1172 ± 173
$[0.02, 0.04]$	999 ± 99
$[0.04, 0.06]$	540 ± 69
$[0.06, 0.08]$	299 ± 54
$[0.08, 0.10]$	225 ± 44
$[0.10, 0.20]$	454 ± 64
$[0.20, 0.30]$	47 ± 34

for the expected resolution of λ^M, and G is a Gaussian function $G(\lambda^M - \lambda, \sigma, s) = 1/(\sqrt{2\pi}\sigma s)\exp[-(\lambda_M - \lambda)^2/(2\sigma^2 s^2)]$. Here, σ is the decay length uncertainty, which is determined for each candidate from the track parameter uncertainties propagated to the vertex uncertainties.

To determine $f_{\rm res}(\sigma)$, signal and background subsamples are defined according to the mass of the $K^0_S p$ system. All events with $2244.7 < M(K^0_S p) < 2326.9$ MeV/c^2 are included in the signal subsample, and all events with $2183.9 < M(K^0_S p) < 2225.0$ MeV/c^2 and $2346.6 < M(K^0_S p) < 2387.7$ MeV/c^2 are included in the background subsample. In addition, the events in both subsamples are required to have a measured proper decay length exceeding 200 μm. This cut reduces the background under the Λ_c^+ signal and the contribution of peaking background. The $f_{\rm res}(\sigma)$ distribution is obtained by subtracting the distribution of expected resolution in the background subsample from the distribution in the signal subsample, and the integration in the definition of $R(\lambda^M - \lambda, s)$ is replaced by the sum over the bins of the $f_{\rm res}(\sigma)$ distribution.

The Λ_b^0 lifetime is determined by the minimization of $\chi^2 = \sum_i^{N_{\rm bins}} (n_i - n_i^e)^2/\sigma_i^2$, where the sum is taken over all bins of measured proper decay length (Table I). The free parameters of the fit are $N_{\rm tot}$, $\tau(\Lambda_b^0)$ and $r_{\rm bck}$. A separate study is performed to measure the resolution scale factor using the decay $D^{*+} \to D^0\pi^+$ with $D^0 \to \mu^+\nu K^0_S\pi^-$. It has a similar topology to that of the $\Lambda_b^0 \to \mu\bar{\nu}\Lambda_c^+$ decay. Since the D^{*+} meson comes mainly from $c\bar{c}$ production, its decay vertex coincides with the primary interaction point. The distribution of the D^{*+} proper decay length is mainly determined by the detector resolution and can be used to measure the resolution scale factor. A value of 1.19 ± 0.06 is found. The scale factor in the lifetime fit is fixed to this value and varied later in a wide range to estimate an associated systematic uncertainty.

The lifetime fit gives $\tau(\Lambda_b^0) = 1.290^{+0.119}_{-0.110}$(stat) ps, and the fraction of peaking background $r_{\rm bck} = 0.160^{+0.068}_{-0.074}$(stat). Figure 2 shows the distribution of the number of $\Lambda_c^+\mu$ events versus λ^M together with the result of the lifetime fit superimposed. The lifetime model agrees well with data with a χ^2/d.o.f. $= 5.5/7$. The dashed line shows separately the contribution of the peaking background.

The method used to fit the mass distribution in each of the λ^M bins is the most significant source of systematic uncertainty. The fit sensitivity is tested by refitting each λ^M bin for the mass interval between 2.17 and 2.40 GeV/c^2 with a linear parametrization of the background. Binning effects of the mass histograms are checked by performing fits to the data with bins of half the nominal width and with the lowest and highest bins excluded. The lifetime fit is performed again for each test. The largest deviation of $\tau(\Lambda_b^0)$ is 0.067 ps, which is given as the systematic uncertainty due to the mass-fitting procedure. The parameters

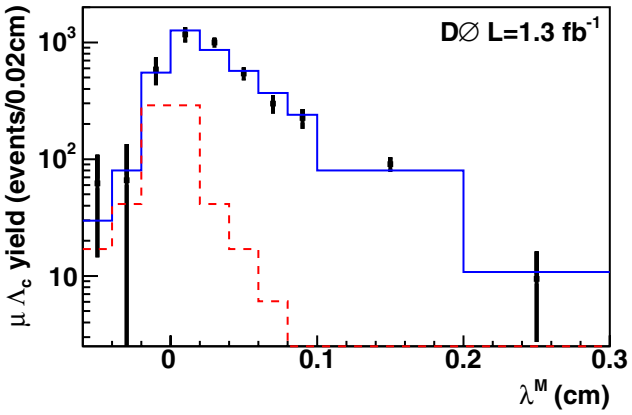

FIG. 2 (color online). Measured $\mu\Lambda_c^+$ yields in the λ^M bins (points) and the result of the lifetime fit (solid histogram). The dashed histogram shows the contribution of the peaking background. In each of the last two bins, the total yield is as shown in Table I.

describing the peaking background are varied by their uncertainties, giving a shift of 0.012 ps in the Λ_b^0 lifetime.

The selected sample can also contain a contribution from $B \to \mu\bar{\nu}\Lambda_c^+ X$ decay. Its branching fraction is unknown; only the upper limit $\mathrm{Br}(B \to e\bar{\nu}\Lambda_c^+ X) < 3.2 \times 10^{-3}$ at 90% C.L. is available [5]. The possible contamination from this decay would reduce the fitted Λ_b^0 lifetime, since the K factor for these events is smaller. The upper 90% C.L. limit on the fraction of this decay in the selected sample is estimated to be 5%, which would result in the reduction of the Λ_b^0 lifetime by 0.027 ps.

The value of the scale factor is varied by $\pm 20\%$, and shifts of approximately ± 0.036 ps are observed in the fitted lifetime. This value is also included in the systematic uncertainty. The overall systematic uncertainty due to the K factor distribution is estimated to be 0.036 ps. It includes the uncertainty in the fraction of $\Lambda_b^0 \to \mu\bar{\nu}\Lambda_c^+$ decay in semileptonic Λ_b^0 decays, the dependence of the K factor on the muon momentum and the uncertainty in generation and decay of Λ_b^0 hadrons [16,17]. The effect on lifetime measurement due to misalignment of elements of the tracking detector is determined by rescaling the geometrical position of all detectors within uncertainties of the alignment procedure. The resulting variation of the Λ_b^0 lifetime is estimated to be 0.018 ps.

The total systematic uncertainty of this measurement is estimated to be $^{+0.087}_{-0.091}$ ps.

Extensive consistency checks using the simulation demonstrate that this analysis gives an unbiased measurement of the Λ_b^0 lifetime and the correct statistical uncertainty. We also split the data sample into two roughly equal parts using various criteria and measure the Λ_b^0 lifetime in each sample independently. The sample is split according to the muon charge, the muon direction, the K^0_S decay length or

the chronological date of data taking. All such tests give statistically consistent values of the Λ_b^0 lifetime.

In conclusion, our measurement of the Λ_b^0 lifetime using the semileptonic decay $\Lambda_b^0 \to \mu\bar{\nu}\Lambda_c^+ X$ results in $\tau(\Lambda_b^0) = 1.290^{+0.119}_{-0.110}(\text{stat})^{+0.087}_{-0.091}(\text{syst})$ ps. It is consistent with the current world average Λ_b^0 lifetime and with our measurement in the exclusive decay $\Lambda_b^0 \to J/\psi\Lambda$ [7]. These two D0 results are statistically independent and the correlation of known systematic effects between them is small. Their combination results in $\tau(\Lambda_b^0) = 1.251^{+0.102}_{-0.096}$ ps.

We thank the staffs at Fermilab and collaborating institutions, and acknowledge support from the DOE and NSF (USA); CEA and CNRS/IN2P3 (France); FASI, Rosatom and RFBR (Russia); CAPES, CNPq, FAPERJ, FAPESP and FUNDUNESP (Brazil); DAE and DST (India); Colciencias (Colombia); CONACyT (Mexico); KRF and KOSEF (Korea); CONICET and UBACyT (Argentina); FOM (The Netherlands); Science and Technology Facilities Council (United Kingdom); MSMT and GACR (Czech Republic); CRC Program, CFI, NSERC and WestGrid Project (Canada); BMBF and DFG (Germany); SFI (Ireland); The Swedish Research Council (Sweden); CAS and CNSF (China); Alexander von Humboldt Foundation; and the Marie Curie Program.

[*]Visiting scientist from Augustana College, Sioux Falls, SD, USA.
[†]Visiting scientist from The University of Liverpool, Liverpool, United Kingdom.
[‡]Visiting scientist from ICN-UNAM, Mexico City, Mexico.
[§]Visiting scientist from Helsinki Institute of Physics, Helsinki, Finland.
[‖]Visiting scientist from Universität Zürich, Zürich, Switzerland.

[1] M. Neubert and C. T. Sachrajda, Nucl. Phys. **B483**, 339 (1997).
[2] M. Di Pierro *et al.*, Phys. Lett. B **468**, 143 (1999).
[3] E. Franco *et al.*, Nucl. Phys. **B633**, 212 (2002).
[4] F. Gabbiani *et al.*, Phys. Rev. D **70**, 094031 (2004).
[5] W.-M. Yao *et al.* (Particle Data Group), J. Phys. G **33**, 1 (2006).
[6] A. Abulencia *et al.* (CDF Collaboration), Phys. Rev. Lett. **98**, 122001 (2007).
[7] V. Abazov *et al.* (D0 Collaboration), Phys. Rev. Lett. **99**, 142001 (2007).
[8] V. Abazov *et al.* (D0 Collaboration), Nucl. Instrum. Methods Phys. Res., Sect. A **565**, 463 (2006).
[9] V. Abazov *et al.*, Nucl. Instrum. Methods Phys. Res., Sect. A **552**, 372 (2005).
[10] D. J. Lange, Nucl. Instrum. Methods Phys. Res., Sect. A **462**, 152 (2001).
[11] T. Sjöstrand *et al.*, Comput. Phys. Commun. **135**, 238 (2001).
[12] CERN Program Library Long Writeup Report No. W5013, 1993; documentation available at http://wwwasd.web.cern.ch/wwwasd/geant/.
[13] S. Catani, Yu. L. Dokshitzer, M. Olsson, G. Turnock, and B. R. Webber, Phys. Lett. B **269**, 432 (1991).
[14] J. Abdallah *et al.* (DELPHI Collaboration), Eur. Phys. J. C **32**, 185 (2004).
[15] G. Borisov, Nucl. Instrum. Methods Phys. Res., Sect. A **417**, 384 (1998).
[16] V. Abazov *et al.* (D0 Collaboration), Phys. Rev. Lett. **94**, 182001 (2005).
[17] V. Abazov *et al.* (D0 Collaboration), Phys. Rev. Lett. **97**, 021802 (2006).